



Charge/Discharge Mechanism of Multicomponent Olivine Cathode for Lithium Rechargeable Batteries

Young-Uk Park^a, R. A. Shakoor^b, Kyu-Young Park^b and Kisuk Kang^{a,†}

^aDepartment of Materials Science and Engineering, Seoul National University, Gwanak-ro 1, Gwanak-gu, Seoul 151-742, Korea

^bDepartment of Materials Science and Engineering and KAIST Institute for Eco-Energy, KAIST, Gwahangno 335, Yuseong-gu, Daejeon 305-701, Korea

ABSTRACT:

Quasi-equilibrium profiles are analyzed through galvanostatic intermittent titration technique (GITT) and potentiostatic intermittent titration technique (PITT) to study the charge/discharge mechanism in multicomponent olivine structure ($\text{LiMn}_{1/3}\text{Fe}_{1/3}\text{Co}_{1/3}\text{PO}_4$). From GITT data, the degree of polarization is evaluated for the three regions corresponding to the redox couples of $\text{Mn}^{2+}/\text{Mn}^{3+}$, $\text{Fe}^{2+}/\text{Fe}^{3+}$ and $\text{Co}^{2+}/\text{Co}^{3+}$. From PITT data, the current vs. time responses are examined in each titration step to find out the mode of lithium de-intercalation/intercalation process. Furthermore, lithium diffusivities at specific compositions (x in $\text{Li}_x\text{Mn}_{1/3}\text{Fe}_{1/3}\text{Co}_{1/3}\text{PO}_4$) are also calculated. Finally, total capacity (Q^{total}) and diffusional capacity (Q^{diff}) are obtained for some selected voltage steps. The entire study consistently confirms that the charge/discharge mechanism of multicomponent olivine cathode is associated with a one-phase reaction rather than a biphasic reaction.

Keywords: Multicomponent olivine cathode, GITT, PITT, Cottrell-type, One-phase reaction

Received December 17, 2010 : Accepted February 27, 2011

1. Introduction

A considerable attention has been focused to control the environmental pollution and depletion of oil resources. A promising suggested solution has led to the development of eco-friendly vehicles that use the “green” energy storage, systems such as plug-in hybrid electric vehicles (PHEVs) and hybrid electric vehicles (HEVs). The launch of PHEVs and HEVs has opened a new chapter to develop such a high performance cathodes which can fulfill their challenging requirements such as high stability, high energy density, high power and low cost.¹⁻⁷⁾ An extensive research has been underway since long to meet the future challenges of energy storage devices. In this context, the lithium transition metal phosphate, LiMPO_4 (where $M = \text{Mn, Fe, Co, or Ni}$) having olivine structure, has been

attracting a lot of attention. The LiMPO_4 is considered as one of the most promising cathode materials and has some prominent advantages over the current cathode material (LiCoO_2) such as remarkably stability even in harsh operating conditions, nontoxic, and potentially inexpensive.⁸⁾ Besides these advantages, these materials are suffering from some short comings. For instance, LiFePO_4 is suffering from low energy density which is essentially due to its low equilibrium potential; LiMnPO_4 is severely affected by the sluggish kinetics of lithium diffusion and LiCoPO_4 is suffering from the low activity because of high redox potential of cobalt. In order to overcome the limitations of each individual transition metal phosphate, recently a multicomponent system has been proposed where Fe, Mn and Co has been affectively combined to form a homogeneous solid solution.^{2,9,10)} It has been demonstrated through experiments and first-principles calculations that each transition metal retains its original identity and shares its role in electrochemical activity unlike their single compo-

[†]Corresponding author. Tel.: +82-2-880-7088

E-mail address: matlgen1@snu.ac.kr

nent state. There is increase in redox potential of iron ($3.2 \rightarrow 3.4$ V) and a decrease in the redox couple of cobalt ($4.9 \rightarrow 4.6$ V) is observed thus making them quite useful for practical applications. This shift in redox potential of each transition metal is observed due to the charge redistribution and the relative energy change from the multiple M/Li interactions. In addition, the distribution of multiple transition metals in olivine structure alters local crystal structure and electronic structure, affecting its kinetic and thermodynamic properties. The multicomponent effect also reduces the Jahn-Teller effect of Mn and significantly enhances both Li mobility and electron (polaron) conductivity. Interestingly, it has been demonstrated that the multicomponent olivine structure exhibits one phase reaction during intercalation/de-intercalation of lithium. The unexpected one-phase Li insertion/extraction reaction of the multicomponent olivine cathode has been explained with respect to the multiple interactions of M/Li or M/vacancy ($M = \text{transition metals}$).^{2,9,10}

The purpose of this report is twofold. Firstly, a study on the charge/discharge mechanism will help to fully understand the unique features associated with multicomponent system. Secondly, this will further validate our previous reported results related to the exhibition of one-phase reaction during intercalation/de-interaction of lithium into/from the host structure (solid solution formation). We believe that complete understanding of charge/discharge mechanism will also provide an opportunity to develop/modify better cathode materials in future for energy storage devices.

2. Experimental

2.1. Preparation of multicomponent olivine, $\text{LiMn}_{1/3}\text{Fe}_{1/3}\text{Co}_{1/3}\text{PO}_4$

A mixed transition metal oxalate, $\text{Mn}_{1/3}\text{Fe}_{1/3}\text{Co}_{1/3}(\text{C}_2\text{O}_4)_2 \cdot 2\text{H}_2\text{O}$, were prepared in optimized coprecipitation condition described at.¹⁰ Sulfate sources of $\text{MnSO}_4 \cdot \text{H}_2\text{O}$ (99%, Aldrich), $(\text{NH}_4)_2\text{Fe}(\text{SO}_4)_2 \cdot 6\text{H}_2\text{O}$ (99%, Aldrich), $\text{CoSO}_4 \cdot 7\text{H}_2\text{O}$ (99%, Aldrich), and ammonium oxalate $((\text{NH}_4)_2\text{C}_2\text{O}_4 \cdot \text{H}_2\text{O}$, 99%, Aldrich) with a molar ratio of 1 : 1 : 1 : 3 were used as precursors. We prepared two different aqueous solutions: (i) 0.7 M mixed transition metal sulfate solution and (ii) 0.5 M ammonium oxalate solution. The former was added drop wise to the latter with stirring. The coprecipitation reaction was continued for 2 hours in Ar-filled glove box to keep the oxidation state of each transition metal +2. The temperature of a reaction bath was maintained at 90°C, and the coprecipitated solution was aged in an argon atmosphere for 7 hours to obtain

a phase-pure mixed a-oxalate. After precipitation and cooling, the precipitate was separated and washed with DI water several times using a centrifuge. The separated precipitate was dried at 70°C in a vacuum oven for 10 hours. The multi-component olivine $\text{LiMn}_{1/3}\text{Fe}_{1/3}\text{Co}_{1/3}\text{PO}_4$ was synthesized by a solid-state reaction using LiH_2PO_4 (97%, Alfa Aesar) and the mixed transition metal oxalate, $\text{Mn}_{1/3}\text{Fe}_{1/3}\text{Co}_{1/3}(\text{C}_2\text{O}_4)_2 \cdot 2\text{H}_2\text{O}$ with a molar ratio of 1 : 1. Pyromellitic acid hydrate, 6 wt%, (PA, 99%, Fluka) was added as an organic additive. The mixture was wet ball-milled using acetone for 18 hours. After evaporating the acetone, the mixture was heated at 500°C for 10 hours under argon flow. The calcined sample was cooled to room temperature and reground. Additionally, 6 wt% PA as an organic additive and 1 wt% ferrocene (98%, Aldrich) as a graphitization catalyst were added to carbon-coat the material. This whole mixture was ball-milled again in acetone media for 2 hours. After evaporating the acetone, the mixture was pelletized manually under 200 kg cm^{-2} pressure using a disk-shape mould. The pellets were heated again sintered at 600 °C for 10 hours under argon flow, cooled to room temperature, and finally ground. XRD spectra and SEM images of the mixed transition metal oxalate and the resulting multicomponent olivine are presented in Fig. 3 and Fig. 5 at,¹⁰ respectively.

2.2. Electrochemical tests

For the electrochemical characterization, a slurry of 79 wt% $\text{LiMn}_{1/3}\text{Fe}_{1/3}\text{Co}_{1/3}\text{PO}_4$, 12 wt% carbon black and 9 wt% polyvinylidene fluoride (PVDF) dispersed in N-methyl-2-pyrrolidone (NMP) was prepared. The slurry was casted on aluminum foils using a doctor-blade. The casted electrodes were dried at 110 °C for 2 hours in air to evaporate NMP and the electrodes of desired size were punched. CR2016 type coin-cells were assembled in an Ar-filled glove box using punched electrodes as a cathode, Li as a counter electrode, Celgard 2400 as a separator and 1 M solution of LiPF_6 in a mixture of ethyl carbonate/dimethyl carbonate (EC/DMC, 1 : 1 v/v) as an electrolyte. The electrochemical properties were examined with the help of a battery cycler (WonA Tech, WBCS 3000, Korea). Galvanostatic intermittent titration technique (GITT) measurement was performed by using a constant current of C/50. The electrochemical cells were charged and discharged for 1 hour at C/50 rate with 2 hours rest time in galvanostatic mode. Potentiostatic intermittent titration technique (PITT) measurement was also carried out by using a “staircase” voltage profile in which the cell potential was increased in 5 mV increments, and the

current vs time, $I(t)$, was measured at each constant potential step. Each individual titration was finished when the absolute current reached a $C/50$ rate. The voltage range for GITT and PITT measurement was 2.0–4.9 V.

3. Results and Discussion

The electrochemical activity of each redox couple ($\text{Mn}^{2+}/\text{Mn}^{3+}$, $\text{Fe}^{2+}/\text{Fe}^{3+}$, or $\text{Co}^{2+}/\text{Co}^{3+}$) the $\text{LiMn}_{1/3}\text{Fe}_{1/3}\text{Co}_{1/3}\text{PO}_4$ electrode was investigated by galvanostatic intermittent titration technique (GITT). The variation of voltage with time was recorded and then converted to the V vs. x curve as shown in Fig. 1, where V is the cell voltage and x is the number of lithium in the olivine structure. Almost 0.84 Li was extracted from the olivine structure during charging, and 0.72 Li was intercalated to the structure during discharging. Three slopping regions were observed in both charge and discharge profiles, implying that three different redox couples contribute to the capacity. The values of voltage at the end of each rest step in GITT measurement generally indicate the quasi-equilibrium voltage at that composition.^{11–13)} Therefore, the dashed line in Fig. 1 indicates the quasi-equilibrium charge/discharge profile of multicomponent olivine, and the extent of deviation from this profile represent the degree of polarization at that composition. A careful analysis of Fig. 1 indicates that almost no polarization is observed for all the three redox couples during charging. However, upon discharging, second region in discharge profile shows relatively large polarization, implying that the $\text{Mn}^{3+}/\text{Mn}^{2+}$ redox couple is kinetically very sluggish especially during the discharge process. This observation

is well consistent with previous reports which mention the much slow kinetics of Mn during discharging.¹⁴⁾ Furthermore, the quasi-equilibrium charge/discharge profile is quite slopping, giving us a hint that the charge/discharge mechanism of the multicomponent olivine is based on a solid solution de/intercalation process rather than a biphasic process. The biphasic process has been reported as the general insertion mechanism in single component olivine cathodes, LiMPO_4 ($M = \text{Mn, Fe, or Co}$).¹⁵⁾

The best way to determine the nature (one-phase vs. two-phase) of the insertion process is the PITT measurement. In the PITT measurement, the current vs. time, $I(t)$, is measured for each voltage step indicative of each composition. Generally, the character of the current vs. time response, $I(t)$, gives useful information about charge/discharge mechanism.^{11–13)} Basically, there are two different types of I - t curves in PITT measurement, one is “Bell-shape” which has local maximum value of current for each individual titration and the other one is “Cottrel-type” in which the current abruptly decays with time for each voltage step. “Bell-shape” I - t curve in PITT measurement is representative of de-intercalation/interaction of lithium in the structure based on the nucleation and growth limited transformation (so called two-phase reaction), whereas a “Cottrel-type” I - t curve in PITT measurement is indicative of the diffusion limited insertion process (so called one-phase reaction).^{16–20)}

Fig. 2(a) represents the I - t curves of $\text{LiMn}_{1/3}\text{Fe}_{1/3}\text{Co}_{1/3}\text{PO}_4$ in PITT measurement. It can be noticed that there is no presence of local maxima throughout the whole region of charge and discharge which implies that the I - t curve do not follow the “Bell-shape”. On the other hand, the current decays rapidly with time, confirming the “Cottrel-type” and hence proving that the de-intercalation/interaction of Li in multicomponent olivine ($\text{LiMn}_{1/3}\text{Fe}_{1/3}\text{Co}_{1/3}\text{PO}_4$) is associated with diffusion limited insertion process. “Cottrel-type” can be also verified more precisely by another plot, $1/(I(t)t)$ versus $1/t$. Fig. 2(b) shows analysis of potentiostatic responses for six selected voltage steps indicated in Fig. 2(a). A regression on a plot of $1/(I(t)t)$ versus $1/t$ shows a linear relationship which means an almost complete lithium solid solution. The good linear fit in the whole voltage regions during charging and discharging indicates mainly diffusion limited responses (Cottrellian behaviors) across the entire charge and discharge ranges.^{21–22)}

In addition, the voltage curves from the PITT measurement as a quasi-equilibrium profile have three slopping regions rather than three voltage plateaus. This is also in

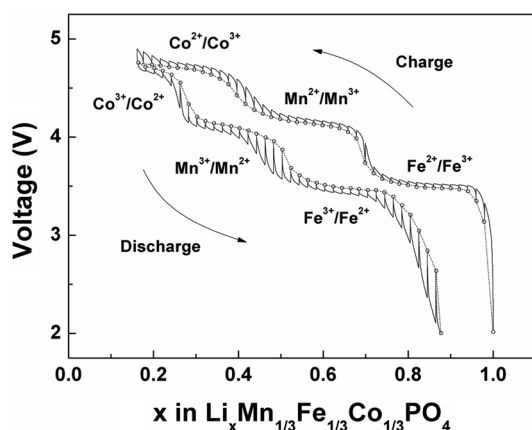


Fig. 1. GITT curve for multicomponent olivine cathode in charging and discharging mode.

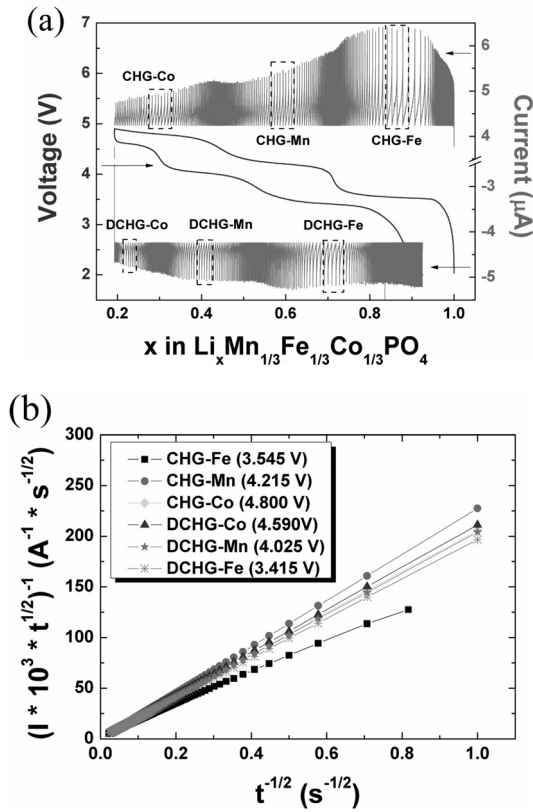


Fig. 2. (a) PITT curve for the multicomponent olivine cathode in charging and discharging mode. (b) Analysis of potentiostatic responses for six selected voltage steps indicated in (a). Plots of $1/(I(t)t)$ versus $1/t$ show the good fit to linearity for all selected voltage steps, implying diffusion limited responses (Cottrellian behaviors) for the entire state-of-charge range.

good agreement with GITT measurement, and indicates that charge/discharge mechanism of multicomponent olivine cathode is one-phase mode rather than two-phase mode.

Lithium diffusivities or chemical diffusion coefficients can be calculated using Cottrell's diffusion-only model by applying to the PITT data.^{21,22} The detailed methods to extract lithium diffusivities from PITT data can be found elsewhere.²⁰ Fig. 3 (a and b) shows the variation of lithium diffusivity with the composition calculated from the PITT measurement during charge and discharge. Diffusivity is in the range of 10^{-9} – 10^{-12} $\text{cm}^2 \text{s}^{-1}$. Three minima of lithium diffusivity correspond to three sloping regions related to three redox couples ($\text{Mn}^{2+}/\text{Mn}^{3+}$, $\text{Fe}^{2+}/\text{Fe}^{3+}$, and $\text{Co}^{2+}/\text{Co}^{3+}$). The D vs. x profile of charge and discharge has three depressed regions, and their shape is

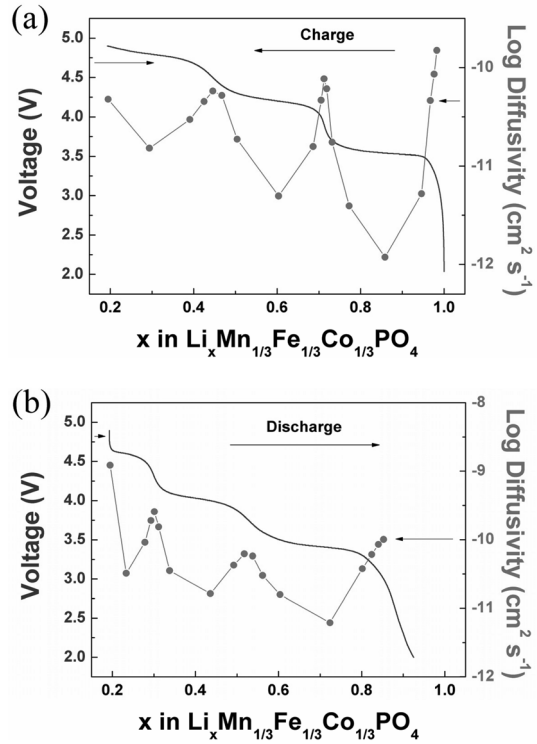


Fig. 3. Variation of lithium diffusivities with the composition calculated from the PITT measurement during (a) charge and (b) discharge. Voltage profiles as the composition is also represented with diffusivity for comparison.

fairly smooth rather than sharp, implying that lithium insertion mechanism is related to solid solution and one-phase behavior.

Fig. 4 shows total capacity, Q^{total} (filled bars), and “diffusive” capacity, fQ^{total} or Q^{diff} (patterned bars) measured upon charge and discharge. The detailed methods to calculate Q^{total} and Q^{diff} from the PITT data are described elsewhere.^[20] It can be noticed from the Fig. 4 that the f values ($Q^{\text{diff}} / Q^{\text{total}}$) which correspond to the fractions of the diffusional contributions to the whole capacity are almost unity in all range of charge and discharge. This behavior indicates that the lithium transport process is mainly diffusion-controlled rather than nucleation and growth limited transformation in the whole range. This is one of the strong evidences which confirm that the insertion/de-insertion mechanism of lithium into/from $\text{LiMn}_{1/3}\text{Fe}_{1/3}\text{Co}_{1/3}\text{PO}_4$ is associated with a one-phase reaction.

Fig. 5 shows the lithium diffusivities and the capacities, Q^{total} , versus the voltage at which the $I(t)$ response was

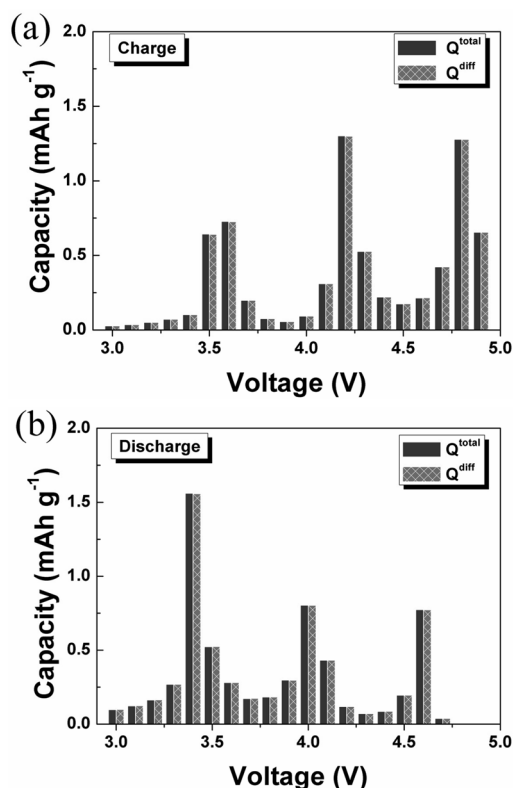


Fig. 4. Total capacity, Q^{total} (filled bars), and “diffusive” capacity, Q^{diff} (patterned bars) measured upon (a) charge and (b) discharge.

measured. It can be seen that the maximum capacity is delivered at the voltage which corresponds to the minimum value of the lithium diffusivity. In addition, the yielded capacities are widely distributed over the whole voltage range rather than concentrated at very narrow voltage window, implying that the miscibility gap or solid solution region is wide. This result also confirms that the charge/discharge mechanism of the multicomponent olivine cathode is governed by one-phase reaction over the entire voltage range.

4. Conclusion

Quasi-equilibrium profiles of $\text{LiMn}_{1/3}\text{Fe}_{1/3}\text{Co}_{1/3}\text{PO}_4$ were investigated during charging and discharging through GITT and PITT measurements. The resultant profiles showed three different quite slopping regions indicating the formation of a solid solution. The “Cottrell-type” I - t curve during PITT measurement confirms that

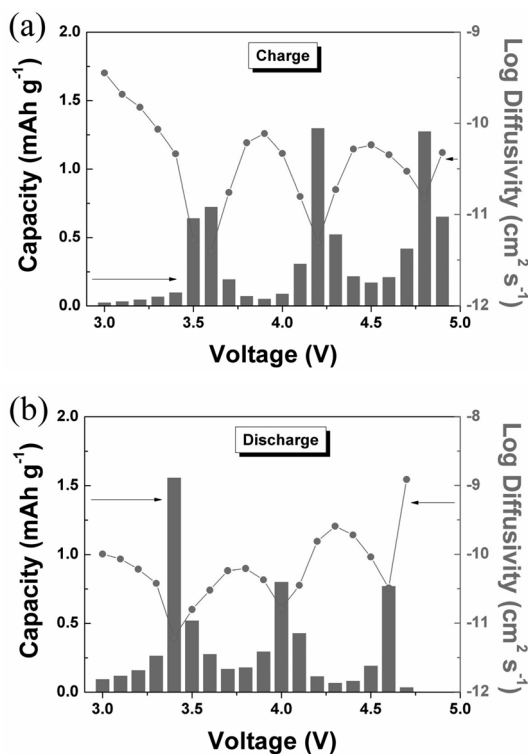


Fig. 5. Diffusivities obtained from PITT data plotted against the voltage at which the $I(t)$ response was measured upon (a) charge and (b) discharge. Superimposed against the diffusivity are the specific capacities, Q^{total} , measured at the same potential upon (a) charge and (b) discharge, respectively.

the de-intercalation/interaction of Li in multicomponent olivine ($\text{LiMn}_{1/3}\text{Fe}_{1/3}\text{Co}_{1/3}\text{PO}_4$) is associated with diffusion limited insertion process (so called one-phase reaction). In addition, in PITT measurement, the conservation of the lowest values of chemical diffusion coefficients at three depressed regions and the unit value of ($Q^{\text{diff}}/Q^{\text{total}}$) confirms that the charge/discharge mechanism of multicomponent olivine cathode is governed by one-phase or solid solution reaction rather than biphasic reaction.

Acknowledgements

This research was supported by Energy Resources Technology R&D program (20092020100040) under the Ministry of Knowledge Economy, Republic of Korea.

References

1. J. Kim, D.-H. Seo, S.-W. Kim, Y.-U. Park and K. Kang, *Chem. Commun.*, **46**, 1305 (2010).

2. D.-H. Seo, H. Gwon, S.-W. Kim, J. Kim and K. Kang, *Chem. Mater.*, **22**, 518 (2010).
3. K. Kang, Y. Shirely, M.J. Berger, C.P. Grey and G. Ceder, *Science*, **311**, 977 (2006).
4. X.L. Wu, L.Y. Jiang, F.F. Cao, Y.G. Guo and L.J. Wan, *Adv. Mater.*, **21**, 2710 (2009).
5. M. Armand and J.-M. Tarascon, *Nature*, **451**, 652 (2008).
6. T. Jiang, G. Chen, A. Li, C. Wang and Y. Wei, *J. Alloys Compd.*, **478**, 604 (2009).
7. B.L. Ellis, W.R.M. Makahnouk, Y. Makimura, K. Toghill and L.F. Nazar, *Nat. Mater.*, **6**, 749 (2007).
8. M.S. Whittingham, *Chem. Rev.*, **104**, 4271 (2004).
9. H. Gwon, D.-H. Seo, S.-W. Kim, J. Kim and K. Kang, *Adv. Funct. Mater.*, **19**, 3285 (2009).
10. Y.-U. Park, J. Kim, H. Gwon, D.-H. Seo, S.-W. Kim and K. Kang, *Chem. Mater.*, **22**, 2573 (2010).
11. M. Seman, J. Marino, W. Yang and C.A. Wolden, *J. Non-Cryst. Solids*, **351**, 1987 (2005).
12. T. Nishina, H. Ura and I. Uchida, *J. Electrochem. Soc.*, **144**, 1273 (1997).
13. C.J. Wen, B.A. Boukamp, R.A. Huggins and W. Weppner, *J. Electrochem. Soc.*, **126**, 2258 (1979).
14. C. Delacourt, P. Poizot, M. Morcrette, J.-M. Tarascon and C. Masquelier, *Chem. Mater.*, **16**, 93 (2004).
15. A.K. Padhi, K.S. Nanjundaswamy and J.B. Goodenough, *J. Electrochem. Soc.*, **144**, 1188 (1997).
16. N. Meethong, H.-Y. Huang, S.A. Speakman, W.C. Carter and Y.-M. Chiang, *Adv. Funct. Mater.*, **17**, 1115 (2007).
17. N. Meethong, H.-Y. Huang, W.C. Carter and Y.-M. Chiang, *Electrochem. Solid-State Lett.*, **10**, A134 (2007).
18. N. Meethong, Y.-H. Kao, M. Tang, H.-Y. Huang, W.C. Carter and Y.-M. Chiang, *Chem. Mater.*, **20**, 6189 (2008).
19. N. Meethong, Y.-H. Kao, S.A. Speakman and Y.-M. Chiang, *Adv. Funct. Mater.*, **19**, 1060 (2009).
20. N. Meethong, Y.-H. Kao, W.C. Carter and Y.-M. Chiang, *Chem. Mater.*, **22**, 1088 (2010).
21. M.A. Vorotyntsev, M.D. Levi and D. Aurbach, *J. Electroanal. Chem.*, **572**, 299 (2004).
22. M.D. Levi, R. Demadrille, A. Pron, M.A. Vorotyntsev, Y. Gofer and D. Aurbach, *J. Electrochem. Soc.*, **153**, E61 (2005).